DNA-embedded Au/Ag core–shell nanoparticles†

Dong-Kwon Lim, In-Jung Kim and Jwa-Min Nam*

Received (in Cambridge, UK) 16th June 2008, Accepted 23rd July 2008
First published as an Advance Article on the web 15th Septembet 2008
DOI: 10.1039/b810195g

Here, we synthesized highly stable DNA-embedded Au/Ag core–shell nanoparticles (NPs) by a straightforward silver-staining of DNA-modified Au nanoparticles (AuNPs); unlike conventional DNA-surface modified NPs that present particle stability issues, DNA-embedded core–shell NPs offer an extraordinary stability with nanoscale controllability of silver shell thickness; these DNA-embedded core–shell NPs show excellent biorecognition properties and Ag shell-thickness-based optical properties, distinctively different from those of a mixture of AuNPs and AgNPs or Ag/Au alloy nanoparticles.

Bioconjugated gold and silver nanoparticles (AuNPs and AgNPs) have been heavily used in single-component forms (*e.g.* oligonucleotide-modified AuNPs) or multi-component forms (*e.g.* Ag/Au core–shell NPs) for various biosensor[1–9] and programmed material assembly applications.[10,11] For the successful and wide application of these nanomaterials, it is critical to have handles to control size, shape[12–14] and assembly of these metal nanoparticles, to retain the stability of bioconjugated nanoparticles under various conditions (*e.g.* large NP size, high temperature, high salt concentration, *etc.*),[15,16] and to develop a synthetic strategy that does not require complex reaction conditions and instrumentations. Multi-component core–shell NPs (*e.g.* Au/AgNPs or Ag/AuNPs) could find more diverse applications than single-component NPs (*e.g.* AuNPs or AgNPs) because these multi-component particles offer more handles in controlling material structure and properties and allow both the Au and Ag components to be taken advantage of. Among Au and Ag-based core–shell NPs, the use of Au/Ag core–shell NPs[17] would be more beneficial than Ag/Au core–shell NPs[7] because the Ag component with stronger optical properties is in the outer layer in Au/Ag NPs (the extinction coefficient of AgNPs could be ~4 times larger than that of AuNPs of the same size and shape). However, the applications of these Au/Ag core–shell NPs have not been explored well because bioconjugated Ag surfaces are, in general, much less stable than bioconjugated Au surfaces. It often requires multi-thiol anchors to obtain stable DNA-modified AgNPs.[15,16]

Here, we synthesized a series of highly stable DNA-embedded Au/Ag core–shell nanoparticles (DNA-em-Au/AgNPs) with distinctive optical properties using a well-known silver-staining method[18] (Fig. 1). DNA is embedded here, rather than surface-modified, to increase particle stability. By finely controlling the stoichiometry of silver-staining reagents, reaction conditions, and DNA sequence design, biologically functional DNA-em-Au/AgNPs with a few nm Ag shell thickness were obtained. We used these DNA-embedded core–shell NPs for DNA hybridization-based NP assembly applications to show these particles are biologically functional after silver shell growth on DNA-modified AuNP surface. In our scheme, mono-thiolated DNA with the spacer sequence (A_{10}-PEG) was first modified to AuNP. Then, hydroquinone-based nanoparticle-promoted silver(I) reduction chemistry was used to grow a silver nanoshell on the oligonucleotide-modified AuNP. By properly designing the spacer sequence and silver-staining conditions, one could control the thickness of the silver shell along with the optical properties without losing the biorecognition properties of modified DNA (Fig. 1). Importantly, because DNA is embedded in the silver nanoshell rather than modified to the NP surface, DNA–Au/AgNPs are highly stable under various conditions (*e.g.* high salt concentration or high temperature). Further, DNA-em-Au/AgNPs exhibit unique optical properties, different from those of gold and silver nanoparticles. Finally, we showed the use of these DNA-em-Au/AgNPs in DNA detection applications. Experimental results proved that DNA-em-Au/AgNP probes can recognize target DNA to form aggregated DNA-em-Au/AgNPs and subsequently induce color change from orange to dark blue.

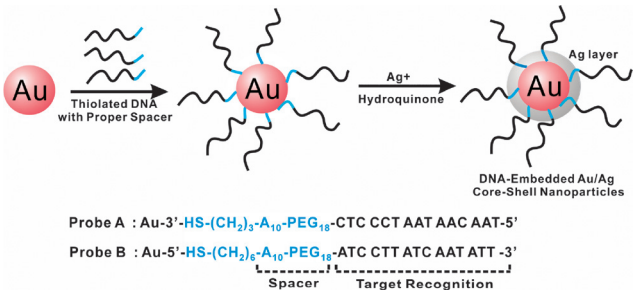

Fig. 1 A schematic illustration of the synthesis of DNA-embedded Au/Ag core–shell nanoparticles.

The silver(I) reduction-based Ag shell growth rate on AuNP is highly dependent on the initial concentration of AuNPs and the amount of silver-staining reagent (1 : 1 mixture of hydroquinone and $AgNO_3$ solutions). If these are not well controlled, the nanoparticles rapidly grow into anisotropic microparticles with excess unreacted silver-staining reagents,[19] and modified oligonucleotides will be buried within the Ag layer and lose their biorecognition properties. For the preparation of DNA-em-Au/AgNPs, first, thiolated oligonucleotides were modified to AuNPs probes (probes A and B in Fig. 1) using a literature method.[20] The A_{10}-polyethylene glycol parts in DNA sequences (blue colored sequences in Fig. 1) work as spacers to give enough space for the silver shell to grow on the AuNP without covering target recognition sequences. Thiolated oligonucleotides (4 nmol) were added to 1 ml of 3.8 nM 15 nm AuNP solution. The solution was then adjusted to obtain DNA-modified AuNPs in 0.3 M phosphate buffered saline (PBS) solution with 0.1% SDS

Department of Chemistry, Seoul National University, 599 Gwanak-ro, Gwanak gu, Seoul, 151-747, South Korea. E-mail: jmnam@snu.ac.kr; Fax: (+82) 2-889-1568

† Electronic supplementary information (ESI) available: Experimental details and UV-visible absorption spectra. See DOI: 10.1039/b810195g

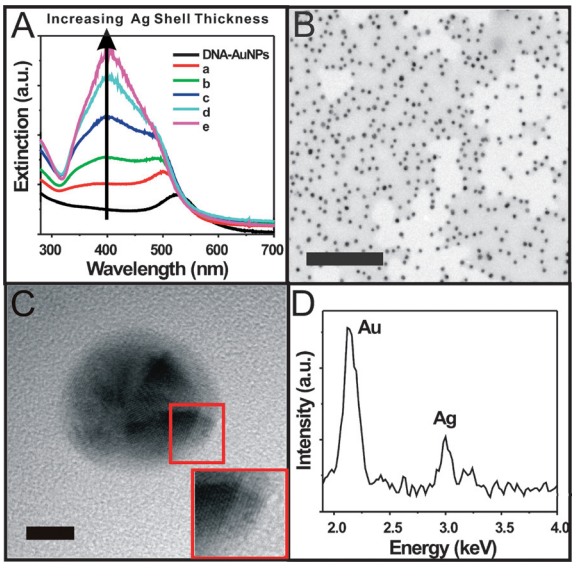

Fig. 2 DNA-em-Au/Ag core–shell nanoparticles. (A) UV-visible spectral profile of DNA-em-Au/Ag core–shell nanoparticle solutions with varying amounts of hydroquinone and $AgNO_3$. Please see the text above for quantitative details for a–e. (B) TEM image (scale bar = 200 nm). (C) HR-TEM images of a DNA-embedded Au/Ag core–shell nanoparticle (scale bar = 5 nm, λ_{max} = 500 nm). (D) Energy-dispersive X-ray (EDX) microanalysis.

at pH 7.4. To remove unreacted thiolated DNA, the solution was centrifuged (14 000 rpm, 15 min), the supernatant was removed, and the precipitate was dispersed in 0.3 M PBS solution (this process was repeated twice). The DNA-modified AuNPs in 0.3 M PBS were then characterized using a UV-visible spectrophotometer (DNA AuNPs in Fig. 2A). Next, hydroquinone solution [diluted 10 times with water prior to use; 1.2 μl (Fig. 2A-a), 2.0 μl (Fig. 2A-b), 2.4 μl (Fig. 2A-c), 3.2 μl (Fig. 2A-d), and 4.0 μl (Fig. 2A-e)] was added to 1 ml of oligonucleotide-modified AuNPs (1 nM, 0.3 M PBS, pH = 7.4). After a brief mixing, $AgNO_3$ solution [diluted 10 times with water prior to use; 1.2 μl (Fig. 2A-a), 2.0 μl (Fig. 2A-b), 2.4 μl (Fig. 2A-c), 3.2 μl (Fig. 2A-d), and 4.0 μl (Fig. 2A-e)] was rapidly added. The solution was vigorously mixed and incubated at room temperature. The reaction progress was monitored every 5 min by UV-visible spectroscopy. The reaction was accompanied by a solution color change from red wine to orange. In general, it takes 30 min to reach the point with no further change in the UV profile (see ESI, Fig. S1†). Next, the resulting particles were centrifuged (14 000 rpm, 15 min), the supernatant was removed, and the precipitated particles were redispersed in 0.3 M PBS solution (no aggregation was observed). As shown in the UV-visible spectra (Fig. 2A), the thickness of the Ag shell is proportional to the amount of added silver-staining solution. As the Ag shell got thicker, the surface plasmon resonance band of the DNA-em-Au/AgNPs shifted to a shorter wavelength and the silver plasmon band became dominant at ~400 nm (Fig. 2Aa-e). Unlike Au–Ag alloy nanoparticles with a single absorption peak between 393 nm and 505 nm depending on the molar ratio of Au and Ag, the core–shell NPs have two distinct plasmon absorption bands, and their relative intensities depend on the thickness of the shell.[21–23] We further characterized DNA-em-Au/AgNPs, synthesized with 2.0 μl of silver-staining solution (Fig. 2A-b). The TEM image shows that the particles are well-dispersed with uniform size distribution (16.4 ± 2.6 nm) (Fig. 2B). The HR-TEM image of a silver-coated DNA-modified AuNP (Fig. 2C) also shows an increased diameter relative to that of DNA-modified AuNP (from 15 nm to ~16.4 nm in diameter). Fig. 2C shows the difference in electron density for one particle where the Au core is darker than the less dense Ag shell.[21] The magnified HR-TEM image (Fig. 2C, inset) shows distinct lattice patterns, indicative of the crystalline nature of silver shell. The Au : Ag ratio in the core–shell particle was determined to be 7 : 3 by EDX microanalysis (Fig. 2D). Such a ratio corresponds to an Ag shell thickness of ~0.7 nm, which equates to ~3 Ag atom layers (one atomic layer = 2.36 Å[24]). Because the length of the spacer [$(CH_3)_6A_{10}PEG_{18}$] is approximately <9.8 nm, which is longer than the silver shell thickness, it is highly likely that the silver shell does not cover the target recognition sequence.

Fig. 3 shows that the synthesized particles are not a mixture of AgNPs and AuNPs. A simple mixture of 15 nm AgNPs and 15 nm AuNPs exhibits their unique absorption peaks at 400 nm, 520 nm, respectively (Fig. 3A). However, the DNA-em-Au/AgNPs show one main peak at ~500 nm with a broad shoulder around <400 nm. TLC spots further prove that these DNA-em-Au/AgNPs are different from a mixture of AuNPs and AgNPs (Fig. 3B). These features provide strong evidence for the successful formation of silver nanoshells on the surface of oligonucleotide-modified AuNPs. Importantly, synthesized Au/Ag core–shell NPs are substantially stable over one month in a 0.3 M PBS solution at room temperature or even at 70 °C [Fig. 3A inset].

Finally, we used these DNA-embedded core–shell NPs (probe A and B in Fig. 4) for DNA detection. For this experiment, the core–shell particles were synthesized with 2.0 μl of hydroquinone solution and 2.0 μl of $AgNO_3$ solution (Fig. 2A-b). Two DNA-em-Au/AgNP probes (1.5 pmol in 300 μl of 0.3 M PBS solution for probe A and 1.5 pmol in 375 μl of 0.3 M PBS solution for probe B) were mixed, and 6.0 μl of 10 μM target DNA was added to the probe solution (Fig. 4A). The solution was heated to 70 °C above the melting temperature (T_m = 53 °C) and slowly brought

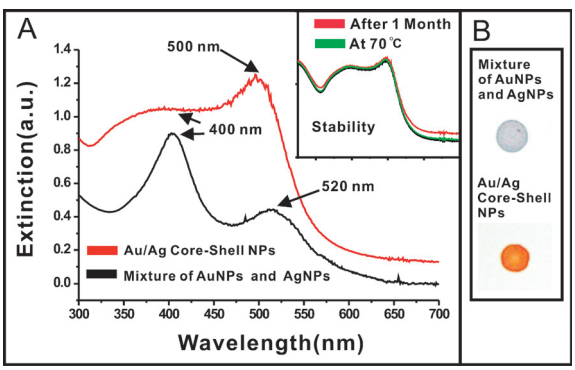

Fig. 3 UV-visible absorption spectra and TLC spots for Au/Ag core–shell NPs and a mixture of AuNPs and AgNPs. (A) UV-visible spectra of a mixture of the same amount of AgNPs (15 nm) and AuNPs (15 nm) (black line) and oligonucleotide-embedded core–shell Au/AgNPs (red line). Inset: stability of DNA-em-Au/Ag core–shell NPs after 1 month at ambient temperature (red line) and at elevated temperature (70 °C, green line). (B) Thin-layer chromatography (TLC) spots of a mixture of AgNPs and AuNPs and DNA-em-Au/AgNPs.

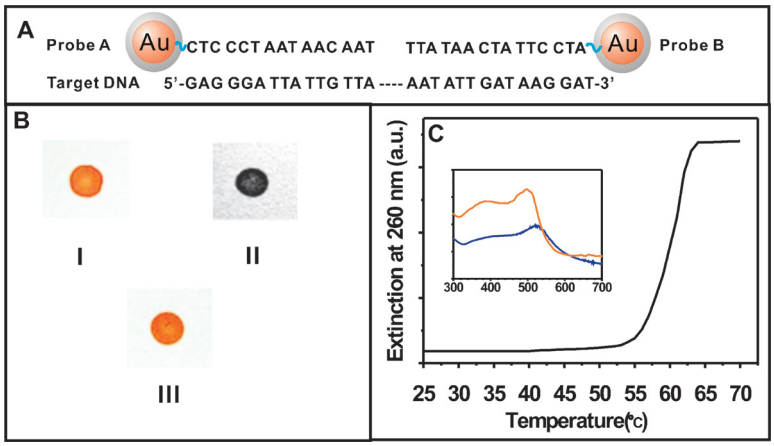

Fig. 4 Target DNA hybridization experiments. (A) DNA-em-Au/AgNP probes and target DNA sequence. (B) TLC spotting of DNA-em-Au/AgNPs before target DNA hybridization (I), DNA-em-Au/AgNPs after target DNA hybridization (II), and DNA-em-Au/AgNPs after dehybridizing target DNA (III). (C) Thermal denaturation curve of DNA-em-Au/AgNP probe aggregates with target DNA as a function of temperature. Inset: UV-visible spectra of DNA-em-Au/AgNPs with target DNA (blue line) and without target DNA (red line).

down to room temperature. After two hours, the formation of nanoparticle aggregates was observed (orange to dark blue color change). 2 μL of the nanoparticles before and after DNA hybridization were spotted respectively onto a C18 reserved-phase TLC plate (Fig. 4B-I and II). UV-visible spectroscopy shows a red shift and dampening of the plasmon resonance spectrum of the core–shell nanoparticles upon target DNA hybridization (Fig. 4C inset). When heated above the melting temperature, the aggregates were disassembled[25] (Fig. 4B-III), and a sharp melting transition was observed (Fig. 4C). Neither aggregation nor change in UV-visible profile were observed with a mismatched, non-complementary sequence (5′-AATATTGATAAGGATTAGGAATAGTTATAA-3′). These results show the oligonucleotide-embedded on Au/Ag core–shell is properly functioning as a nucleic acid nanoprobe and there is no substantial damage to modified DNA during the silver-staining process.

In summary, we developed a straightforward, room temperature synthetic method of obtaining highly stable DNA-em-Au/Ag core–shell nanoparticles based on direct silver-staining of DNA-modified AuNPs. This synthetic strategy does not require any complex experimental setup, high temperature, or long synthesis time. The resultant DNA-embedded core–shell nanoparticles exhibited excellent stability and DNA hybridization/dehybridization capability along with optical properties, distinctively different from those of silver or gold nanoparticles. We showed that, by controlling the amount of silver-staining solution, AuNP seed concentration, and other reaction conditions, the thickness of the silver layer on the gold core can be controlled on a nanometre scale. With proper design of spacer sequence and silver shell thickness, one can retain both DNA detection capability and very good stability under high temperature (>70 °C) and high salt concentration (>0.3 M). This approach could be used to generate various bio-functional Au/Ag core–shell nanoparticles with high stability, high sensitivity, and tailorable optical properties in a straightforward and combinatorial fashion. Applications of these new nanostructures can be easily extended to various biosensing systems (*e.g.* colorimetric bio-detection and Raman-based sensors[2,17]) and programmed nanostructure assemblies.[10,11]

This work was supported by 21C Frontier Functional Proteomics Project (FPR08-A2-150), Nano R&D program (2008-02890) through the Korea Science and Engineering Foundation from Ministry of Education, Science and Technology, and the Seoul R&BD Program (11001 and CR070027).

Notes and references

1 C. Sonnichsen and A. P. Alivisatos, *Nano Lett.*, 2005, **5**(3), 301.
2 C. Y. W. Cao, R. Jin and C. A. Mirkin, *Science*, 2002, **297**, 1536.
3 H. F. Wang, T. B. Huff and D. A. Zweifel, *Proc. Natl. Acad. Sci. U. S. A.*, 2005, **102**, 15752.
4 I. H. El-Sayed, X. H. Huang and M. A. El-Sayed, *Nano Lett.*, 2005, **5**, 829.
5 C. D. Medley, J. E. Smith, Z. Tang, Y. Wu, S. Bamrungsap and W. Tan, *Anal. Chem.*, 2008, **80**, 1067.
6 J.-M. Nam, S. I. Stoeva and C. A. Mirkin, *J. Am. Chem. Soc.*, 2004, **126**, 5932.
7 Y. W. Cao, R. Jin and C. A. Mirkin, *J. Am. Chem. Soc.*, 2001, **123**, 7961.
8 J. J. Storhoff, A. D. Lucas, V. Garimella, Y. P. Bao and U. R. Muller, *Nat. Biotechnol.*, 2004, **22**, 883.
9 C. Agbasi-Porter, J. Ryman-Rasmussen, S. Franzen and D. L. Feldheim, *Bioconjugate Chem.*, 2006, **17**(5), 1178.
10 D. Nykypanchuk, M. M. Maye, D. Lelie and O. Gang, *Nature*, 2008, **451**, 549.
11 S. Y. Park, A. K. R. Lytton-Jean, B. Lee, S. Weigand, G. C. Schatz and C. A. Mirkin, *Nature*, 2008, **451**, 553.
12 A. R. Tao, S. Habas and P. Yang, *Small*, 2008, **4**(3), 310.
13 C. L. Nehl, H. Liao and J. H. Hafner, *Nano Lett.*, 2006, **6**(4), 683.
14 B. J. Wiley, Y. Xiong, Z.-Y. Li, Y. Yin and Y. Xia, *Nano Lett.*, 2006, **6**(4), 765.
15 J. S. Lee, A. K. R. Lytton-Jean, S. J. Hurst and C. A. Mirkin, *Nano Lett.*, 2007, **7**(7), 2112.
16 Z. Li, R. C. Jin, C. A. Mirkin and R. L. Letsinger, *Nucleic Acids Res.*, 2002, **30**(7), 1558.
17 S. Pande, S. K. Ghosh, S. Praharaj, S. Panigrahi, S. Basu, S. Jana, A. Pal, T. Tsukuda and T. Pal, *J. Phys. Chem. C*, 2007, **111**, 10806.
18 T. A. Taton, C. A. Mirkin and R. L. Letsinger, *Science*, 2000, **289**, 1757–1760.
19 X. Xu, D. G. Georganopoulou, H. D. Hill and C. A. Mirkin, *Anal. Chem.*, 2007, **79**, 6650.
20 J.-M. Nam, K.-J. Jang and J. T. Groves, *Nature Protocols*, 2007, **2**, 1438.
21 R. G. Freeman, M. B. Hommer, K. C. Grabar, M. A. Jackson and M. J. Natan, *J. Phys. Chem.*, 1996, **100**, 718.
22 M. P. Mallin and C. J. Murphy, *Nano Lett.*, 2002, **2**(11), 1235.
23 S. Link, Z. L. Wang and M. A. El-Sayed, *J. Phys. Chem. B*, 1999, **103**, 3529.
24 T. Shibata, B. A. Bunker, Z. Zhang, D. Meisel, C. F. Vardeman II and J. D. Gezelter, *J. Am. Chem. Soc.*, 2002, **124**, 11989.
25 R. Jin, G. Wu, Z. Li, C. A. Mirkin and G. C. Schatz, *J. Am. Chem. Soc.*, 2003, **125**, 1643.